Biol. Cybern. 86, 395–401 (2002)
DOI 10.1007/s00422-001-0304-z

Biological Cybernetics

Nonlinear dynamics of the EEG separated by independent component analysis after sound and light stimulation

Seung-Hyun Jin[1], **Jaeseung Jeong**[2], **Dong-Gyu Jeong**[3], **Dai-Jin Kim**[4], **Soo Yong Kim**[1]

[1] Department of Physics, Korea Advanced Institute of Science and Technology, 373-1 Kusong-dong, Yusong-gu, Taejon 305-701, Korea
[2] National Creative Research Initiative, Center for Neuro dynamics and Department of Physics, Korea University, Seoul 136–701, Korea
[3] Department of Information and Communications Engineering, Woosuk University, Chon-Buk 565-701, Korea
[4] Department of Psychiatry, College of Medicine, The Catholic University of Korea, Seoul, Korea

Received: 12 March 2001 / Accepted in revised form: 27 November 2001

Abstract. The electroencephalogram (EEG) is a multiscaled signal consisting of several time-series components each with different dominant frequency ranges and different origins. Nonlinear measures of the EEG reflect the complexity of the overall EEG, but not of each component in it. The aim of this study is to examine effect of the sound and light (SL) stimulation on the complexity of each component of the EEG. We used independent component analysis to obtain independent components of the EEG. The first positive Lyapunov exponent (L1) was estimated as a nonlinear measure of complexity. Twelve subjects were administered photic and auditory stimuli with a frequency of 10 Hz, which corresponded to the alpha frequency of the EEG, by a sound and light entrainment device. We compared the L1 values of the EEGs and their independent components between baseline and after the SL stimulation. We detected that the L1 values of the EEG decreased after the SL stimulation in all channels except C3 and F4, indicating that the complexity of the EEG decreased. We showed that alpha components increased in proportion but decreased in complexity after the SL stimulation. The beta independent components were found to decrease in proportion and complexity. These results suggest that decreased complexity of the EEG after the SL stimulation may be principally caused by decreased complexity and increased proportion of the alpha independent components. We showed also that theta components increased in complexity after the SL stimulation. We propose that nonlinear dynamical analysis combined with independent component analysis may be helpful in understanding the temporal characteristics of the EEG, which cannot be detected by conventional linear or nonlinear methods.

Correspondence to: S.-H. Jin (e-mail: shjin@cais.kaist.ac.kr), Tel.: +82-42-8692569, Fax: +82-42-8692510

1 Introduction

The electroencephalogram (EEG) is a multiscaled signal which consists of several time-series components with different dominant frequency ranges generated from different sites in the brain. According to the frequency range, it can be conventionally subdivided into delta (1–4 Hz), theta (4–7 Hz), alpha (8–13 Hz), and beta (13–30 Hz) waves. For example, theta rhythm is thought to be produced in the cortical limbic area such as the hippocampus, entorhinal cortex, and cingulate areas, while high-amplitude delta waves are recorded from cortical and thalamic single neurons and complex circuits (Niedermeyer and Lopes da Silva 1993).

However, the estimation of nonlinear dynamical measures of the EEG such as the correlation dimension (D2) and the first positive Lyapunov exponent (L1) cannot detect dynamical properties of each component in the EEG. Rather, they can only detect properties of the summation of the components. The aim of the present study is to investigate nonlinear dynamical properties of the components in the EEG as well as the EEG induced by sound and light (SL) stimulation. We used independent component analysis (ICA) to obtain independent components of the EEG. ICA is an effective algorithm for separating or estimating waveforms of mutually independent components from an array of sensors without knowledge of any characteristics of the transmission channels. Recently ICA has been applied to blind source separation in various fields, in particular EEG, ERP (Event Related Potential) and fMRI (functional Magnetic Resonance Imaging) analyses (Lee 1998).

A sound and light entainment device (SLED) was used to produce the SL stimulation. The SLED entrains brain waves by generating photic and auditory stimuli of a certain frequency. The mechanism of this device is based on the finding by Gray Walter that when a person is subjected to a light flashing at a certain frequency, his or her brain-wave activity falls in to synchronization with the flashing of the lights (Walter and Walter 1949; Walter 1957). SLEDs are currently being used by professional psychologists in their practices and by the

general public for a variety of practical uses, including relaxation, stress management, accelerated learning and retention, sports training, and promoting physical wellness (Green and Green 1986; Lubar 1989; Hutchison 1990). Little is, however, known about the effects of SLED on brain functions and EEG, although there have been several research studies on it. (Van der Tweel and Verduyn Lunel 1965; Hoovey et al. 1972; Townsend 1973; Williams and West 1975; Inouye et al. 1980; Glickson 1986; Richardson and McAndrew 1990; Erol 1999).

In order to investigate the effects of SLEDs on the complexity of the EEG and its independent components, we compared the L1 values of the EEG and the independent components separated by ICA before and after the SL stimulation. In Sect. 2, we briefly explain the algorithm for estimating the L1 using time series and ICA. Section 3 presents the experimental procedure and data acquisition method of this study. The L1 changes of the EEG and its independent components before and after the SL stimulation are presented in Sect. 4. We discuss our results and nonlinear dynamics of the EEG induced by the SL stimulation in Sect. 5.

2 Materials and methods

2.1 The estimation of L1

In nonlinear analysis, we first transform a one-dimensional time-series EEG into a multidimensional phase space. In a hypothetical system governed by n variables, the phase space is n-dimensional. Each state of the system corresponds to a point in phase space whose n coordinates are the values assumed by the governing variables for this specific state. If the system is observed through time, the sequence of points in phase space forms a dynamical trajectory. This trajectory fills a subspace of the phase space called the system's attractor.

The reconstruction of the attractor in the phase space is carried out through the technique of plotting delay coordinates (Takens 1981; Eckmann and Ruelle 1985). Let an observed time series $x(t)$ be the output of a differentiable dynamical system f^t on an m-dimensional manifold $\boldsymbol{M}$. In order to unfold the projection back to a multivariate phase space that is a representation of the original system, the following delay coordinates are used from a single time series $x(t)$ after performing an embedding procedure.

$$X(t) = [x(t), x(t+T), \cdot, x(t+(d-1)T)] \tag{1}$$

where $X(t)$ is one point of the trajectory in the phase space at time $t, x(t+iT)$ are the coordinates in the phase space corresponding to the time-delayed values of the time series, T is the time delay between the points of the time series considered, and d is the embedding dimension.

The choice of an appropriate time delay T and embedding dimension d are important for the success of reconstructing the attractor with finite data. For the time delay T, we used the first local minimum of the average mutual information between the sets of measurement $x(t)$ and $x(t+T)$. Mutual information measures the general dependence of two variables, in contrast to an autocorrelation function which measures only linear dependence (Fraser and Swinney 1986).

We used the minimum (optimal) embedding dimension in the reconstruction procedure. The basic idea for estimating the minimum embedding dimension is that in the passage from dimension d to dimension $d + 1$, one can differentiate between points on the orbit that are true and those that are false neighbors. A false neighbor is defined as a point in the data set that is adjacent only because we are viewing the orbit (the attractor) in too-small an embedding space ($d < d_{\min}$). When we have achieved a large-enough embedding space ($d \geq d_{\min}$), all neighbors of every orbit point within the multivariate phase space will be true neighbors. The detailed algorithm is presented in Jeong et al. (1998). Figure 1 shows the embedding rate as a function of embedding dimension for 16 384 EEG data points at T4 in a normal control. The optimal minimum embedding dimension for calculating the L1 was selected as 11 in this case.

The complex activity of EEG can be quantified by the L1. Lyapunov exponents estimate the mean exponential divergence or convergence of nearby trajectories of the attractor. A system possessing at least one positive Lyapunov exponent is chaotic, reflecting sensitive dependence on the initial conditions (Fell et al. 1993). In our analysis, we regarded the L1 as a measure of complexity or flexibility, instead of using it as an absolute measure to differentiate between periodic, chaotic, or stochastic dynamics.

We used a modified version of the Wolf algorithm (Wolf et al. 1985) and followed a proposal by Frank et al. (1990) to calculate the L1. Essentially, the Wolf algorithm computes the initial vector distance Δi of two nearby points and evolves its length in a certain propagation time. If the vector length Δf between the two points becomes too large, a new reference point is chosen with properties that minimize the replacement length and the orientation change. Then, the two points are evolved again. After m propagation steps, the L1 is obtained from the sum over the logarithm of the ratios of the vector distances divided by the total evolving time:

$$\mathrm{L1} = \frac{1}{m}\sum_{i=1}^{m} \frac{\ln(\Delta f_i)/\Delta i_i}{\mathrm{EVOLV} \cdot \Delta t} \tag{2}$$

where Δt, Δi, and Δf are the sampling interval, the initial, and the final separations between the points in the fiducial trajectory, and those in the nearest-neighbor trajectory separated in time by the ith EVOLV step, respectively (Wolf et al. 1985; Principe and Lo 1991). The EVOLV step is the evolving time step between initial and final separations. By using the weight function proposed by Frank et al. (1990), we improved the L1 estimate by broadening the search to allow replacements to be well-aligned points lying further apart, but still within the region of linear dynamics. This was also presented in our previous paper (Jeong et al. 1998). Nonlinear time-series methods are well reviewed

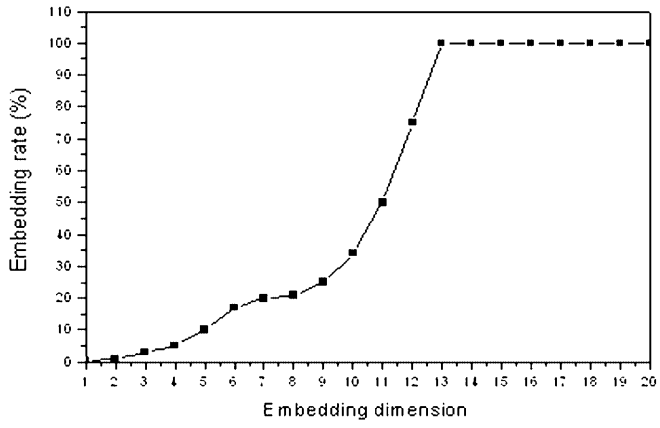

Fig. 1. The embedding rate as a function of embedding dimension for 16 384 EEG data points at T4 in a normal control. The optimal minimum embedding dimension for calculating the first positive Lyapunov exponent (L1) was selected as 11 in this case

in the papers of Grassberger et al. (1991) and Schreiber (1999).

2.2 Independent component analysis

In order to obtain independent components from the EEG, we used the "infomax" algorithm proposed by Bell and Sejnowski (1995). The function of the ICA algorithm is to find a matrix $\mathbf{W}$ which makes the elements $u(t) = [u_1(t), \cdots, u_N(t)]^{\mathrm{T}}$ of the linear transform $u(t) = \mathbf{W}x(t)$ of a data vector $x(t) = [x_1(t), \cdots, x_N(t)]^{\mathrm{T}}$ statistically independent. The number of sources that ICA can separate is equal to the number of channels (sensors). ICA imposes a stronger criterion that the multivariate probability density function of u factorizes: $f_u(u) = \prod_{i=1}^{N} f_{u_i}(u_i)$, whereas decorrelation techniques such as principal component analysis ensure that $\langle u_i u_j \rangle = 0, \forall_{i,j}$. This factorization step involves making the mutual information between u_i go to zero: $I(u_i, u_j) = 0, \forall_{i,j}$ (Comon 1994). Mutual information is a measure of the general dependence of two variables including all higher-order statistics of the u_i, while decorrelation only takes account of linear statistics.

ICA assumes that each of the unknown independent components u_i has the same form of cumulative density function, denoted as $F_u(u)$ after scaling and shifting. ICA can then maximize the entropy $H(\mathbf{y})$ of a nonlinearly transformed vector to minimize the mutual information between $u_i : y = F_u(u)$. This yields stochastic gradient ascent rules for adjusting $\mathbf{W}$:

$$\Delta\mathbf{W} = \varepsilon \frac{\partial H(y)}{\partial \mathbf{W}} \mathbf{W}^{\mathrm{T}}\mathbf{W} = \varepsilon\left[\mathbf{I} - \phi(u)u^{\mathrm{T}}\right]\mathbf{W} \tag{3}$$

where ε is the learning rate (normally less than 0.01) and $\phi(u)$ is the gradient vector of the log likelihood called the "score function" (Amari 1998):

$$\phi(u_i) = \left(\frac{\partial}{\partial u_i}\right) \ln\left(\frac{\partial y_i}{\partial u_i}\right) \tag{4}$$

Practical tests on EEG data showed that the logistic function $y_i = F_{u_i}(u_i) = [1 + \exp(-u_i)]^{-1}$ generated reasonable results compared to other known cumulative density functions (Lee 1998). In the case of $\phi_i(u_i) = 2y_i - 1$, the algorithm has a very simple form. The theory and the practical algorithm of ICA are presented in detail in the papers by the Sejnowski group (Bell and Sejnowski 1995; Makeig et al. 1996; Lee 1998; Lee et al. 2000).

We separated the EEG of each subject into 16 independent components by using ICA, since the number of independent signal sources should be equal to the number of channels. The 16-dimensional vectors were presented to a 16×16 ICA network one at a time. The learning rate was annealed from 0.1 to 0.000001 during the iteration. After each pass through the whole training set, we observed correlation between the ICA output channels and the amount of change in the weight matrix, and stopped the training procedure when the mean correlation among all pairs of the channels was below 0.05 or the ICA weights had stopped changing appreciably. The criteria we used were given by Makeig et al. 1996). We used ICA MATLAB codes provided by the Sejnowski group (http://www.cnl.salk.edu/~tewon/ica_cnl.html).

We categorized each independent component into one of the delta, theta, alpha, and beta independent components, and the noise components according to their dominant frequency and harmonics in the power spectrum. For instance, the alpha independent component is an independent component having a dominant frequency of around 10 Hz (8–13 Hz). Although an independent component has harmonics around 20 Hz, we can distinguish between the alpha and beta components, since the alpha independent component has a larger amplitude in the alpha frequency range around 10 Hz. Some components have broadband spectra that can be considered noise components; these were excluded from the analysis. The theta, delta, and beta independent components are denoted in the same manner. Each independent component was judged by visual inspection of the power spectra by an EEG technician. A similar source distribution of individual independent component estimated by projection maps was also used to confirm the validity of our decision.

The average L1 of independent components within subgroups was used as a measure of complexity of the independent components. For example, we compared the averaged L1 value of the alpha independent components among 16 independent components for individual subjects before SL stimulation with that after the stimulation.

2.3 EEG recording

We used the "MC2 Study α" device, manufactured by Dae-Yang E&C, to generate and present sound and light stimuli. It includes small lights mounted in goggles, which has the advantage that the position of the light sources with respect to the eyes is constant regardless of

head position. A red light (with a mean light intensity of 40 mcd) flashes at 10 Hz and is controlled by a small computer in the base unit. The light source consists of six photodiodes with a peak emission at 650 nm. Three diodes are attached to the center of each eyecup. The light sources are held 1 cm from each eye. Sound is generated at a certain frequency and presented binaurally. Binaural sound occurs when one sine wave (pure tone) is played in one ear, and a different wave is played in the other ear. A subject was stimulated by a 440 Hz tone in one ear and a 430 Hz tone in the other; the ears would hear both tones, but the brain would discern the difference between the 440 Hz and 430 Hz tones (i.e., 10 Hz), which corresponds to the alpha frequency of the EEG.

The subjects consisted of twelve healthy volunteers aged from 13 to 15 years (six females and six males; age = 13.8 ± 0.6 years, mean ± SD). All subjects were right-handed without obvious central nervous system disorders and free of any medication affecting the EEG. They all had used the SLED for 15–30 min daily for the previous 3–6 months.

The first step of the experiment was to let a subject sit comfortably in a sound-proof darkened room. The subject wore the SLED in a relaxed state. The subject was instructed to keep his or her eyes closed during the experiment. We recorded the EEG (5 000 data points) for 10 s as baseline data. The sampling frequency was 500 Hz. The photic and auditory stimuli generated by the SLED were then delivered to the subject for 15 min. The subject could see the red lights even with closed eyes. The second segments of the EEG were recorded just after the SL stimulation for 10 s whilst the subject intained the same physical condition as during the first measurement.

The EEGs were recorded from the 16 scalp loci of the international 10–20 system. The EEG from 16 channels (F7, T3, Fp1, F3, C3, P3, O1, F8, T4, T5, T6, Fp2, F4, C4, P4, and O2) against "linked earlobes" were amplified on a Nihon Kohden EEG-4421K with a time constant of 0.1 s. The sampled data were digitized by a 12-bit analog-to-digital converter in an IBM PC. All data were digitally filtered in order to remove the residual EMG activity at 1–60 Hz. Each EEG record was judged by inspection to be free from electrooculographic and movement artifacts, and to contain minimal electromyographic activity. All recordings were performed in the afternoon to minimize the effects of diurnal variations in arousal level.

3 Results

We defined alpha to beta ratio (α/β) as the ratio of percentage alpha to percentage beta of the power spectrum of the EEG. The α/β may be an effective measure for describing the increase of alpha power and the decrease of beta power of the EEG after the SL stimulation. Table 1 presents the average values and SDs of the α/β before and after the SL stimulation. The average α/β values increased after the SL stimulation at channels Fp1, Fp2, F7, F8, T3, T4, T5, T6, P4, O1, and O2.

The L1s of the EEG recordings from all channels in both states were calculated. We used the time delays of 34–50 ms and embedding dimensions of 11–18 for the delay coordinates. The EVOLV step was selected using the $1/e$ spectral frequency and was about 250 ms. The calculation of the L1 naturally depends on the time over which the trajectory is evaluated. After 200 propagation steps, the values converged around the final value of L1 in an interval of ±1.0%. Figure 1 shows the embedding rate as a function of embedding dimension.

The average L1 values and the SDs in all channels before and after the SL stimulation are summarized in Table 2. It is shown that the L1 values of the EEG at channels Fp1, Fp2, F7, F8, F3, T3, T4, T5, T6, P3, P4, C4, O1, and O2 decreased after the SLED application, indicating that the complexity of the EEG was lowered by the SL stimulation. The differences of the L1 values between two states were 0.05–0.47 bits/s.

ICA was then applied to all EEG recordings. Figure 2 demonstrates a typical example of (a) EEG segments of 10 s from 16 channels and (b) the resulting ICA-transformed EEG time series from a subject after the SLED application. Most independent components have their own characteristic patterns including dominant frequencies, whereas noise components have no distinct dominant frequency.

Figure 3 presents the mean values of the averaged L1s of the delta, theta, alpha, and beta independent components of the EEG before and after the SL stimulation for all subjects. The averaged L1 of the alpha independent wave decreased after the SL stimulation, indicating decreased complexity of the this component (Table 3). The beta independent component also had lowered L1 values after the SL stimulation. One noticeable result was that the complexity of the theta independent com-

Table 1. The average values and SDs of alpha to beta ratio (α/β) in the power spectrum of the EEG before and after the sound and light (SL) stimulation *SLED*, sound and light entrainment device

Channel	Before SLED		After SLED	
	Mean	SD	Mean	SD
F7	3.433	0.449	3.905	0.413
T3	4.394	0.450	4.923	0.479
T5	4.640	0.414	4.676	0.435
Fp1	3.118	0.437	3.185	0.376
F3	4.679	0.374	4.554	0.366
C3	4.553	0.338	4.455	0.414
P3	4.980	0.391	4.863	0.413
O1	4.526	0.323	4.915	0.350
F8	2.305	0.440	2.456	0.433
T4	4.931	0.352	5.323	0.387
T6	4.843	0.376	5.215	0.347
Fp2	2.827	0.418	2.858	0.414
F4	4.484	0.413	4.453	0.383
C4	4.340	0.391	4.324	0.380
P4	4.758	0.417	4.807	0.434
O2	4.725	0.338	5.029	0.345

Table 2. The mean L1 values of the EEG from 16 channels before and after the SL stimulation

Channel	Before SLED		After SLED	
	Mean	SD	Mean	SD
F7	3.424	0.144	2.950	0.149
T3	3.094	0.590	2.870	0.279
T5	3.531	0.181	3.078	0.392
Fp1	3.233	0.316	3.003	0.368
F3	2.730	0.791	2.678	0.365
C3	3.076	0.128	3.453	0.240
P3	3.562	0.349	3.228	0.532
O1	3.421	0.751	3.108	0.276
F8	3.457	0.617	3.170	0.311
T4	3.140	0.371	2.922	0.130
T6	3.154	0.183	2.911	0.465
Fp2	3.205	0.353	3.006	0.197
F4	3.207	0.388	3.350	0.54
C4	3.152	0.328	2.873	0.101
P4	3.581	0.393	3.291	0.383
O2	3.190	0.365	3.050	0.305

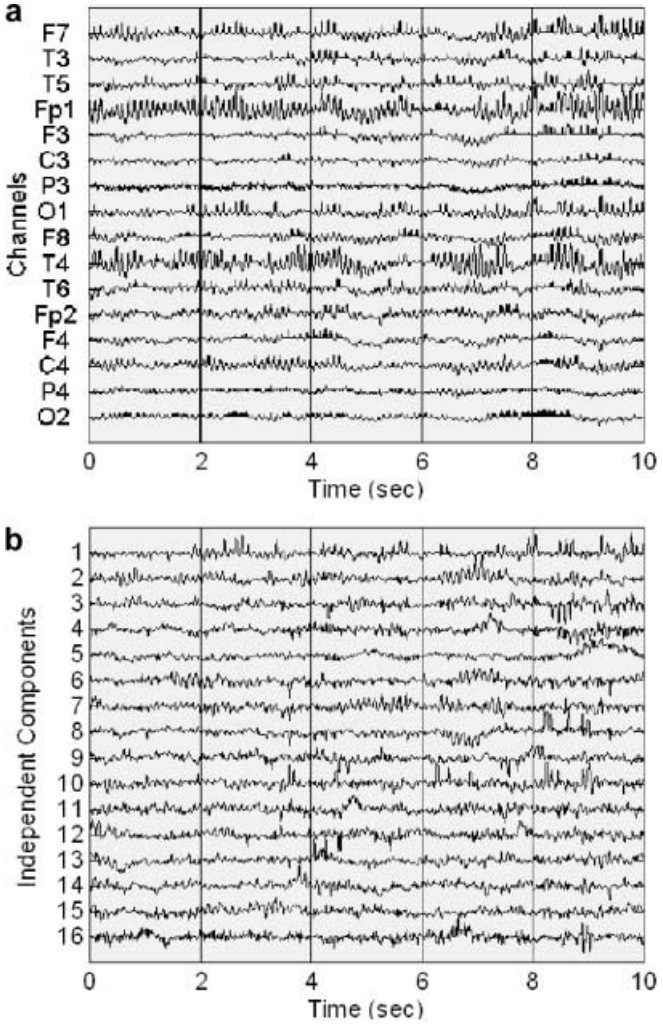

Fig. 2. **a** EEG time series at 16 channels and **b** the resulting independent-component-analysis-transformed EEG time series from a subject after the SL stimulation

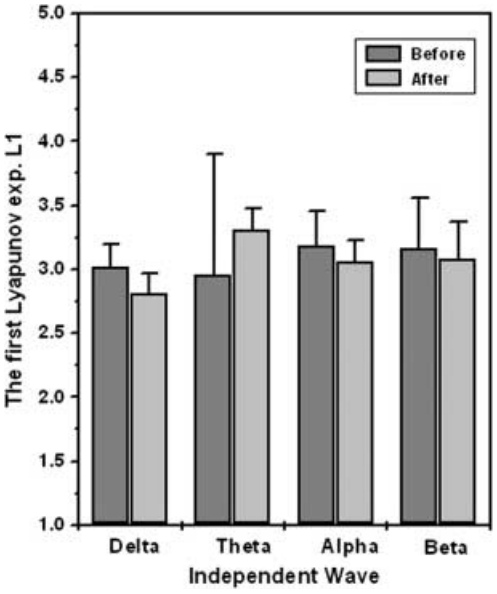

Fig. 3. The comparison of the mean values of the averaged L1 values of the delta, theta, alpha, and beta independent components before and after the SL stimulation

Table 3. The mean values of the averaged L1 values of the delta, theta, alpha, and beta independent components of the EEG before and after the SL stimulation

	Before SLED		After SLED	
	Mean	SD	Mean	SD
Delta	3.014	0.180	2.813	0.157
Theta	2.955	0.942	3.431	0.162
Alpha	3.186	0.269	3.057	0.170
Beta	3.163	0.398	3.076	0.295

ponent induced by SLED increased in complexity. The averaged L1 value for the theta independent component induced by SLED was 0.48 bits/s larger than that for the baseline.

4 Discussion

The results of the present study indicate that the power distribution and complexity of the EEG after the SL stimulation are different from those of the baseline EEG. The percentage alpha of the EEG increased after the SL stimulation, while percentage beta decreased. The EEG induced by the SL stimuli at 10 Hz had decreased L1 values mainly in the temporal and occipital regions, which are associated with the information processing of auditory and photic stimuli, respectively. The averaged L1s of the alpha and beta independent components of the EEG decreased after the SL stimulation, whereas the theta independent component had higher L1 values after the SL stimulation.

The results suggest that decreased complexity of the EEG after the SL stimulation may be principally caused by the increased proportion and decreased complexity of

the alpha independent components. One explanation is that the SL stimuli at alpha frequency give rise to the entrainment of brain waves with alpha waves (like a resonance phenomenon), and collective activation of alpha rhythm generators in the brain, if they exist. The collective activation of alpha rhythms causes the increased proportion of alpha waves to have decreased complexity, which results in the decreased complexity in EEG. Townsend et al. (1975) reported that sine-wave-modulated light stimulation at the subject's alpha frequency imposed phase locking in the cortical alpha rhythm, thus stabilizing the alpha frequency and increasing the alpha amplitude. The decreased complexity of beta waves that resulted from the alpha resonance-like phenomenon induced by SLED may also cause the EEG to be less complex. The cooperative dynamics between independent components will need to be further examined.

We observed an increased complexity of theta independent components after the SL stimulation. Although we do not understand the reason for this, we suggest that the SLED can activate theta rhythm generators such as the hippocampal formation. According to the studies of Klimesch et al. (1994, 1997), EEG theta activity is related to memory processes. They found that theta power was increased during the encoding or retrieval process of episodic information. Bilateral lesion of the hippocampal formation leads to an inability to encode and/or retrieve new episodic information. Although SLEDs have not been proven to enhance the learning and memory functions, they are used currently in many countries (including South Korea) as a device for accelerating learning and memory processes of the brain. Further examination of the dynamics of the theta independent components in future studies may give us clues on the effect of the SLED on learning and memory processes.

EEG changes by photic stimuli have been found to be associated with various cerebral abnormalities (Rodin et al. 1953; Kooi et al. 1957; Kooi and Thomas 1958; Oosterhuis et al. 1969). The light-induced abnormalities have been reported in several mental disorders including depression (Kleiber et al. 1978), anxiety (Ulett et al. 1953) and schizophrenia (Rice et al. 1989). Asymmetry in the photic stimulation is also closely related to the focal slowing and CT scan evidence of parenchymatous brain disease (Coul and Pedley 1978). Thus, light stimulation is commonly used in routine EEG examinations and has proven to be useful in investigating neurological disorders (Takahashi 1989). However, numerous studies have performed only spectral analysis of the EEG induced by photic stimuli (Rice et al. 1989; Jin et al. 1990). Nonlinear methods may be helpful in diagnosing pathological states of the brain.

Our method is a hybrid based on ICA and nonlinear methods. As with any method, our method has certain limitations and difficulties. One of these involves the identification of independent components obtained from ICA. Not all independent components have distinct patterns that can be categorized into delta, theta, alpha, and beta independent components – some of the independent components have mixed dominant frequency ranges and patterns. It is also difficult to differentiate noise signals from high-frequency independent components. Thus, we must establish definite criteria for identifying independent components. Another difficulty is that the number of independent components depends on the number of sensors (channels). Thus, the number of channels may influence the values of the nonlinear measures of the independent components. Therefore, it is also necessary to design an elaborate method for combining nonlinear methods with ICA.

Despite these difficulties, nonlinear analysis of independent components obtained from ICA may be useful for examining the temporal dynamics of the time series consisting of mutually independent components, such as the EEG. Consider, for example, a time series that consists of two independent components of different dimensions, D1 and D2. The dimension of the summed time series D3 gives no information about the dimensions of its components. Hence, the calculation of the nonlinear measures of the independent components requires additional information on each component of the signal.

In our previous studies, we estimated the D2 of the components obtained from band-pass filters in the EEG stimulated by SLED. We found that the average D2 values of the alpha band decreased after the SL stimulation at channels F3, T4, T6, and P4, while the theta band increased at channels P4 and Fp1 (Han et al. 1998). A linear band-pass filtering method gives topological information on the sources of the components, which cannot be obtained from ICA. However, it may lead to the distortion of dynamics and consequently spurious results. In addition, the difference of the results between using the linear band-pass filtering method and ICA may be a result of nonlinear effects of the components. While linear band-pass filters decompose signals into linearly independent components, ICA divides them into nonlinear (higher-order) independent components. We suggest that the nonlinear analysis of the independent components using ICA may be useful in preserving the dynamics of the components and in examining their dynamical properties.

Acknowledgement. This work was partially supported by Dae-Yang E&C and Korea Science and Engineering Foundation.

References

Amari S (1998) Natural gradient works efficiently in learning. Neural Comput 10:251–276

Bell AJ, Sejnowski TJ (1995) An information maximization approach to blind separation and blind deconvolution. Neural Comput 7:1129–1159

Comon P (1994) Independent component analysis – a new concept? Signal Process 36:287–314

Coul B, Pedley T (1978) Intermittent photic stimulation: clinical usefulness on non-convulsive responses. Electroencephalogr Clin Neurophysiol 44:343–363

Eckmann JP, Ruelle D (1985) Ergodic theory of chaos and strange attractors. Rev Mod Phys 57:617–656

Erol B (1999) Brain function and oscillations. II. Integrative brain function. Neurophysiology and cognitive processes. Springer, Berlin Heidelberg, New York, pp 129–142

Fell J, Röschke J, Beckmann P (1993) The calculation of the first positive Lyapunov exponent in sleep EEG data. Electroencephalogr clin Neurophysiol 86:348–352

Frank GW, Lookman T, Nerenberg MAH, Essex C (1990) Chaotic time series analysis of epileptic seizures. Physica D 46:427–438

Fraser AM, Swinney HL (1986) Independent coordinates for strange attractors from mutual information. Phys Rev A 33:1134–1140

Glickson J (1986) Photic driving and altered states of consciousness: an exploratory study. Image Cogn Person 6:167–182

Grassberger P, Schreiber T, Schaffrath C (1991) Nonlinear time sequence analysis. Int J Bifurc Chaos 1:521–547

Green EE, Green AM (1986) Biofeedback and States of Consciousness. In: Wolman BB, Ullman M (eds) Handbook of states of consciousness. Van Nostrand Reinhold, New York

Han S, Jin S-H, Jeong Y, Jeong J, Kim D-J, Kim C-H, Kim C-K, Kim S-Y (1998) Can an alpha-induced stimulator enhance a memory process in the brain? In: Shiro U, Takashi O (eds) Proceedings of the Fifth International Conference on Neural Information Processing. IOS, Ohmsha pp 442–445

Hoovey ZB, Heinemann U, Creutzfeldt OD (1972) Inter-hemispheric synchrony of alpha waves. Electroencephalogr Clin Neurophysiol 32:337–347

Hutchison MA (1990) Time flashes: a short history of light/sound technology. Megabrain Rep 2:2–5

Inouye T, Sumitsuji N, Matsumoto K (1980) EEG changes induced by light stimuli modulated with the subject's alpha rhythms. Electroencephalogr Clin Neurophysiol 49:135–142

Jin Y, Potkin SG, Rice D, Sramek J, Costa J, Isenhart R, Heh C, Sandman CA (1990) Abnormal EEG responses to photic stimulation in schizophrenic patients. Schizophr Bull 16:627–634

Jeong J, Kim SY, Han SH (1998) Nonlinear analysis of the EEG in Alzheimer's disease with optimal embedding dimension. Electroencephalogr Clin Neurophysiol 106:220–228

Kleiber E, Broveman D, Vogel W (1978) Effects of estrogen therapy on plasma MAO activity and EEG driving responses of depressed women. Am J Psychiatry 128:1492–1498

Kliemesch W, Schimke H, Schwaiger J (1994) Episodic and semantic memory: an analysis in the EEG theta and alpha band. Electroencephalogr Clin Neurophysiol 91:428–441

Kliemesch W, Doppelmayr M, Schimke H, Ripper B (1997) Theta synchronization and alpha desynchronization in a memory task. Psychophysiology 34:169–176

Kooi KA, Thomas MH (1958) Electronic analysis of cerebral responses to photic stimulation in patients with brain damage. Electroencephalogr Clin Neurophysiol 10:417–424

Kooi KA, Eckman HG, Thomas MH (1957) Observations on the response to photic stimulation in organic cerebral dysfunction. Electroencephalogr Clin Neurophysiol 9:239–250

Lee T-W (1998) Independent component analysis: theory and applications. kluwer Academic, Boston, pp 27–64

Lee T-W, Girolami M, Bell AJ, Sejnowski TJ (2000) A unifying information-theoretic framework for independent component analysis. Comput Math Appl 31:1–21

Lubar JF (1989) Electroencephalographic biofeedback and neurological applications. In: Basmajian JV (ed) Biofeedback: principles and practice. Williams and Wilkins, New York

Makeig S, Bell AJ, Jung TP, Sejnowski TJ (1996) Independent component analysis of EEG data. In: Mozer M, Hasselmo M (eds). Advances in neural information processing Systems 8. MIT Press, Cambridge, Mass., pp 145–151

Niedermeyer E, Lopes da Silva F (1993) Electroencephalography: basic principles, clinical applications, and related fields, 3rd edn. Williams & Wilkins pp 27–62

Oosterhuis HJGH, Ponsen L, Jonkman EG (1969) The average visual response in patients with cerebrovascular disease. Electroencephalogr Clin Neurophysiol 27:23–24

Principe JC, Lo PC (1991) Towards the determination of the largest Lyapunov exponent of EEG segments. In: Duke DW, Pritchard WS (eds) Proceedings of the Conference on Measuring Chaos in the Human Brain. World Scientific, Singapore, pp 156–166

Rice DM, Potkin SG, Jin Y, Isenhart R, Heh CW, Sramek J, Costa J, Sandman CA (1989) EEG alpha photic driving abnormalities in chronic schizophrenia. Psychiatry Res 30:313–324

Richardson A, McAndrew F (1990) The effects of photic stimulation and private self-consciousness on the complexity of visual imagination imagery. Br J Psychol 81:381–394

Rodin EA, Bickford RG, Svien HJ (1953) Electroencephalographic findings associated with subdural hematoma. Arch Neurol Psychiatry 69:743–755

Schreiber T (1999) Interdisciplinary application of nonlinear time series methods. Phys Rep 308:1–64

Takahashi T (1989) Activation methods. In: Niedermeyer E, Lopes da Silva F (eds) Electroencepahlography: basic principles, clinical applications, and related fields. Urban and Schwarzenberg, Baltimore, pp 209–227

Takens F (1981) Detecting strange attractors in turbulence in dynamical systems and turbulence. Lecture notes in mathematics, Vol 898. Springer, Berlin Heidelberg New York, pp 366–381

Townsend RE (1973) A device for generation and presentation of modulated light stimuli. Electroencephalogr Clin Neurophysiol 34:97–99

Townsend RE, Lubin A, Naitoh P (1975) Stabilization of alpha frequency by sinusoidally modulated light. Electroencephalogr Clin Neurophysiol 39:515–518

Ulett VA, Glesser G, Winokor G (1953) The EEG and reaction to photic stimulation as an index of anxiety proneness. Electroencephalogr Clin Neurophysiol 5:23–37

Van der Tweel LH, Verduyn Lunel HFE (1965) Human visual responses to sinusoidally modulated light. Electroencephalogr Clin Neurophysiol 18:587–598

Walter WG (1957) The living brain. Duckworth, London

Walter VJ, Walter WG (1949) The central effects of rhythmic sensory stimulation. Electroencephalogr Clin Neurophysiol 1:57-86

Williams P, West M (1975) EEG responses to photic stimulation in persons experienced in meditation. Electroencephalogr Clin Neurophysiol 39:519–522

Wolf A, Swift JB, Swinney HL, Vastano JA (1985) Deterministic Lyapunov exponents from a time series. Physica D 16:285–317